Thesis

Rasmus Kjær Høier

September 2018

Contents

Abstract

-Set the stage. ESS and need for neutron detection + energy determination. charectarize detectors with known sources. ToF use in other contexts. In medicine for PET scans. In echolocation used by bats and toothed whales. -Advantages of digital techniques -Results: we can do the same measurements, but switching detectors and using more channels is easier. Varying parameters is easier (Take one dataset and vary parameters in software).

1 Introduction

2 Chapter that explains neutron interaction, tagging and also presents the detectors

2.1 Sources

Actinide/Be I used PuBe (which atomic numbers?)

2.2 Neutron Interactions

2.3 Scintillation light and the detectors

Scintillators are mateirals which produce light when radiation passes through. When choosing a scintillator material one needs to consider timing resolution, recovery time, pulse shape discrimination ability, sensitivity to different particles.

Neutrons are detected when they scatter and knock out a protons, which then ionize the scintillator material. High Z/N ratio in the material is important for neutron detection effeciency.

Gammas on the other hand can interact through compton scattering (which may knock an electron free or leave it in an excited state), pair production and the photoelectric effect[**?**].

The detectors used for the experiments presented in this report are an NE213 liquid scintilator detector and a YAP crystal scintillator detector.

-YAP: The Yap detectors are composed of a Cerium doped Yttrium Aluminium Perovskite crystal monunted on a photomultiplier tube. They are only used to detect gammas in order for timestamps to be extracted for each signal. Thus there is no need for pulse shape discrimination capabilities. The typical yap pulse decays within 50-200 ns, which means that the detector can handle count rates in the low MHz range.

-NE213: The NE213 detector is sensitive to both gammas and neutrons. -gamma interaction -neutron interaction -psd -timestamp

2.4 Neutron Tagging

When working with charged particles the energy can for example be calculated from the way in which in which a particles trajectury is bend in a magnetic field. This approach obviously wont work on neutrons, but for fast neutrons the energy can be found by correlating neutrons with gamma photons, which are produced nearly simultaeously. the detection of the neutron gives the end time of its movement from radioactive source to detector, and the gamma ray is used to calculate the start time, and since fast neutrons, E $\approx$ 1-20 MeV, move at classical speeds, we can use classical mechanics to calculate their energy. Using a beryllium based source such as Plutonium beryllium we get both neutrons

and gammas. The first reaction is as follows:

$$^{238}Pu \rightarrow ^{234} U + \alpha + \gamma_1$$

The alpha particle can then interact with the beryllium producing both a neutron and another gamma in the following series of events:

$$[\alpha + ^9 Be \rightarrow ^{12} C^* + n], \qquad \longrightarrow \qquad [^{12}C^* \rightarrow ^{12} C + \gamma_2]$$

The events all occur on a very short timescale, compared to the time it takes the particles to reach the detectors, so the pairs $\gamma_1 - \gamma_2$ and $n - \gamma_1$ can be considered to be produced simultaneuously.

The lab setup is large compared to the source so we assume the particles to come from a single point.

FIGURE: Schematic drawing of Aquarium setup.

2.5 limitations of precision in neutron tagging

Detector resolution, size of source and detector (particles can hit detectors even when travelling at a slight angle), sampling rate if using digitizer.

3 Analog setup

Signals in the NE213 detector are copied in a fan in fan out module. Two of these signals will be used to acquire longgate and shortgate integrals of the pulses. The third signal from the FIFO module is sent into a constant fraction discriminator, which starts a 50 ns square wave pulse when the cfd threshold is surpassed.

This logic signal is then sent to a latch which switches state. For the next 10 μs, until the latch resets, no signals can pass through the latch. This way only one event is processed at a time. The downside to this is that a certain fraction of events a lost. scalers placed on either side of the latch make it possible to calculate this fraction for a given data set.

The signal is then copied again and reshaped. A 60 ns and a 500 ns square wave is used to define the qdc integration window for two copies of the analog NE213 signal mentioned above. A 150 ns square wave is used to define the integration window for the yap qdc, and another square wave triggers the start of a time of flight tdc.

The stop signal comes from the yap. The yap signals are sent into a linear fifo module, with one outgoing signal sent to a qdc, which triggers on the above mentioned NE213 signal. The other outgoing signal is sent to a cfd where a square pulse of 50 ns is produced. this pulse is then delayed by 300 ns and will act as the stop signal if a start signal is received from the NE213.

3.1 Schematic overview

3.2 QDC

3.3 CFD

3.4 TDC

4 Analog results

Over 4 hours of measurements $17.3 \cdot 10^6$ events were recorded by the analog setup. The immediate output is 4 tdc spectrums Giving the time differences for NE213 hits and the respective YAPs. qdc spectra, one for each yap, and two qdc spectra for the NE213 detector (one longgate and one shortgate).

4.1 YAP QDC spectrum

Write about scattered gammas that are both stop and start signals. Geometry dependent. Analog setup only records when there is a ToF coincidence, so scattered gammas end up dominating the yap qdc spectrum, which leads to the yap closest to the NE213 always having the largest gamma peak in the ToF spectrum. The Digital setup records everything passing the threshold, so by comparing with it we get an idea of the real gamma distrubution.

4.2 NE213 QDC spectrum

The energy registered in the longgate QDC is shown in fig 2. 'A peak is clearly visible at around 4.4 MeV_{ec}. This is the energy of the gammas emmited by the deexciting ^{12}C atoms. —Write about other peak—

4.3 ToF spectrum

-ToF spectrum

4.4 Pulse shape discrimination

4.4.1 Charge comparison method

Since neutrons and gammas interact differently in the NE213 detector their signal has different shape and duration. This makes it possible to discriminate between neutrons and gammas.

4.5 Pulse shape v ToF

5 Digital setup

-technology has improved and prizes lowered. ToF with digitized signals opens new possibilities. Advantage is we have more information to work with (expand).

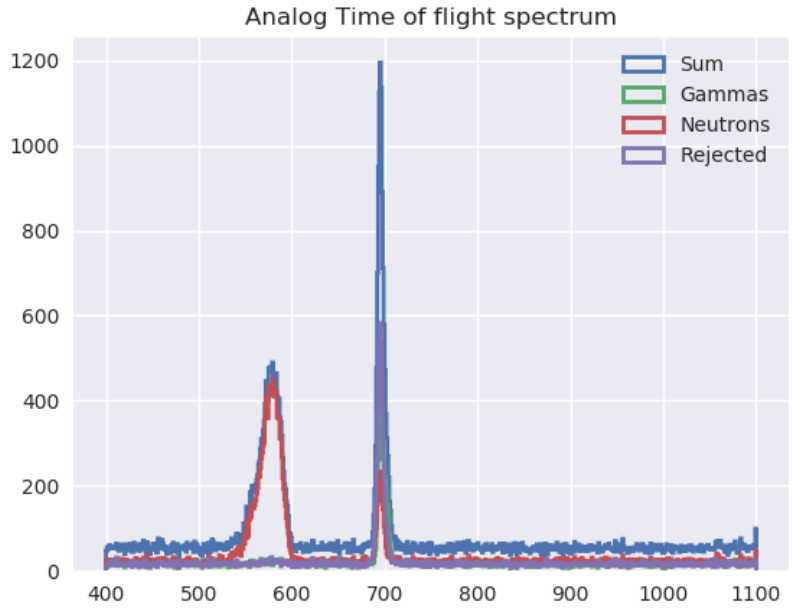

Figure 1: The time of flight spectrum.

disadvantage takes up storage space, but bulk of data can be discarded when desired features are extracted.

6 Digital Results

6.1 -digitizer description + digitizer output description

6.2 -integrating waveforms: QDC spectra

6.3 PSD

PSD from longgate and shortgate integration, filtered time of flight.

6.4 -timestamping: cfd: ToF

The detector signals are led through a patch panel and into an attenuator in order to lower the signal amplitudes. From there they are fed directly into the digitizer. The digitizer will trigger on all enabled channel when the threshold on one channel is surpassed, so a lot of the events will be empty and some will consists of partially contained events. The digitizer used for this project was a a

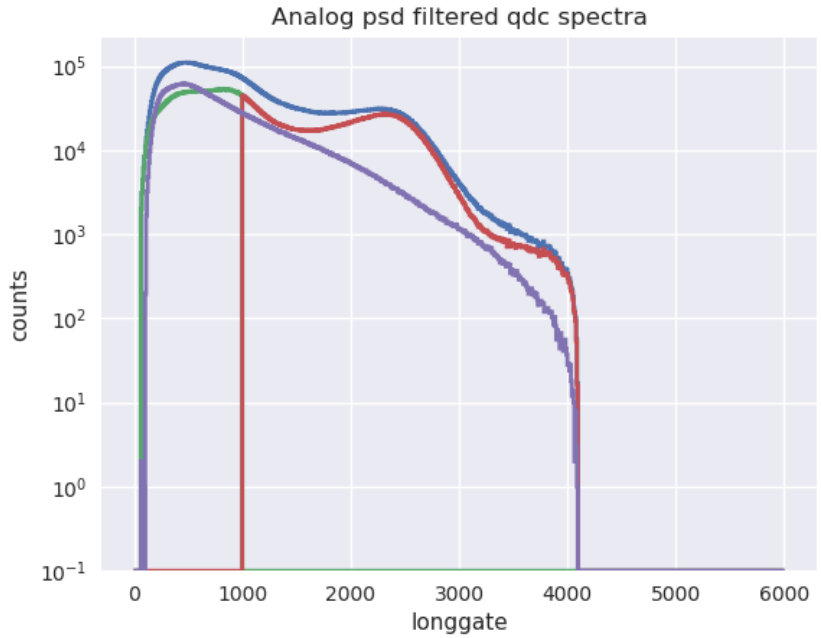

Figure 2: Analog QDC spectrum.

model vx1751 from CAEN, and controlled through the software WaveDumpis. The format of the data is:

{number of samples per window, digitizer model id, Channel number, Event Number, mask, trigger timestamp, DC offset (DAC), samples}

The digitizer triggers on all enabled channels at the same time, so often when a pulse is recorded in one channel nothing an empty sampling window is recorded in the other channels. The data received from the digitizer is processed in order to throw away these empty events, as well as to extract additional features such integrated charge, height, width and a corrected timestamp.

In order to get a good time of flight spectrum we need to have a precise timestamp for each pulse from the detectors. A general timestamp is provided by the digitizer for each event, but a single event may be hundreds or thousands of samples long. For the vc1751 digitizer each sample corresponds to 1 ns, and with detector signals from the NE213 detector and the YAPs ranging from 10-100 ns, then the timestamp needs to be refined.

Fig **??** shows five pulses from the NE213 detector. The approximate location of the pulses in the sampling window can be specified when the digitizer is configured, through the posttrigger parameter. However, this is not very precise, and the pulses may be located several tens of nanoseconds apart.

Aligning pulses by peak height location **??** results in some improvement but

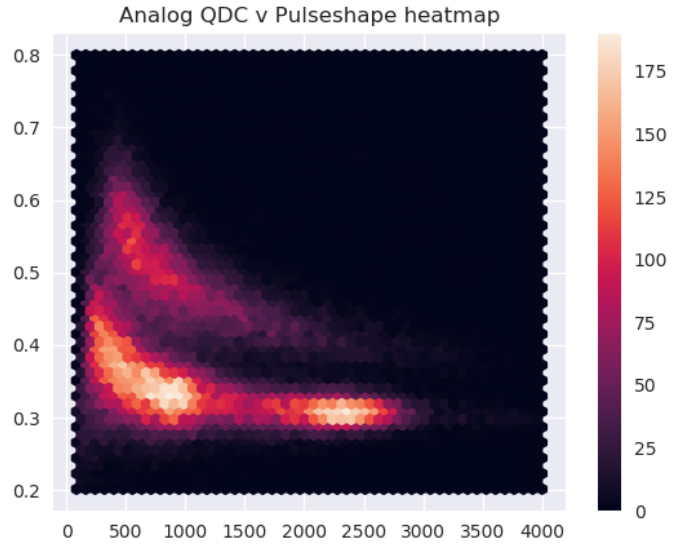

(a) Hexbin heatmap of Pulse shape distribution. The upper band is neutrons and the lower one is gammas.

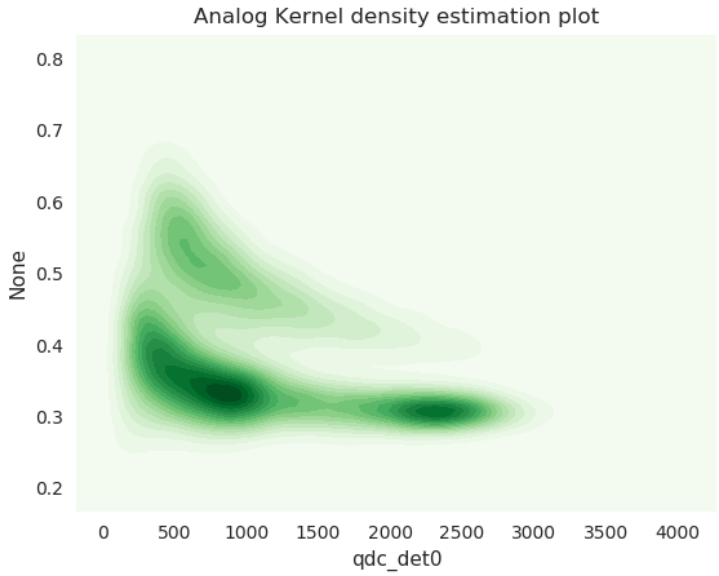

(b) Kernel density estimation plot of the pulse shape spectrum. The upper band is neutrons and the lower one is gammas.

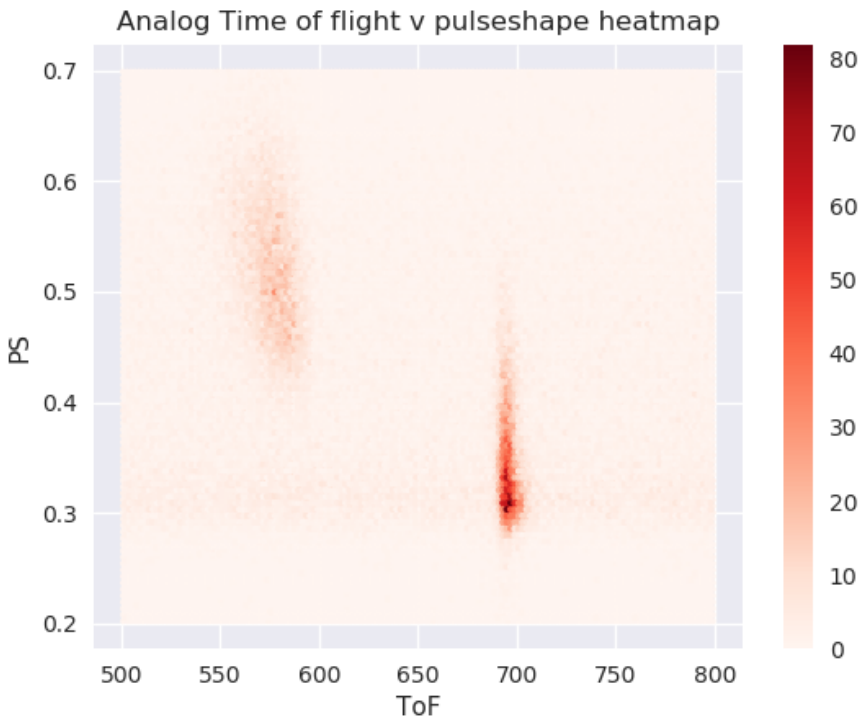

Figure 4: heatmap of ToF vs pulse shape.

also leads to timewalk.

The leading edge method employed to get **??** aligns all pulses around the points where they first surpass a fixed threshold. This method can provide good results provided that the threshold is small compared to the lowest pulseheights.

By using a constant fraction discrimination (cfd) algorithm the five pulses have been aligned in Fig **??**. The cfd algorithm simply scans through an event and locates the first bin to reach a chosen fraction of the pulse's peak value. In Fig **??** 50% of the peak height was used as the constant fraction.

Both the leading edge and the cfd algorithm align all the pulses within one nanosecond of each other. Thus by adding the time value acquired by either of these algorithms we get the precision we need in order to perform time of flight measurements.

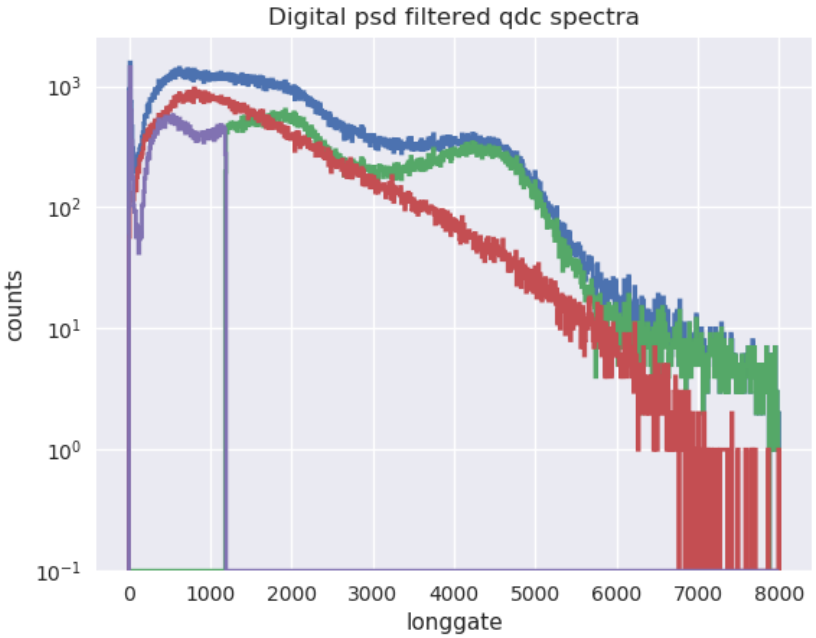

Figure 5: The digital energy spectrum.

6.5 Pulse shape v ToF

6.6 Comparisson between digital and analog results

7 Conclusion

8 Outlook

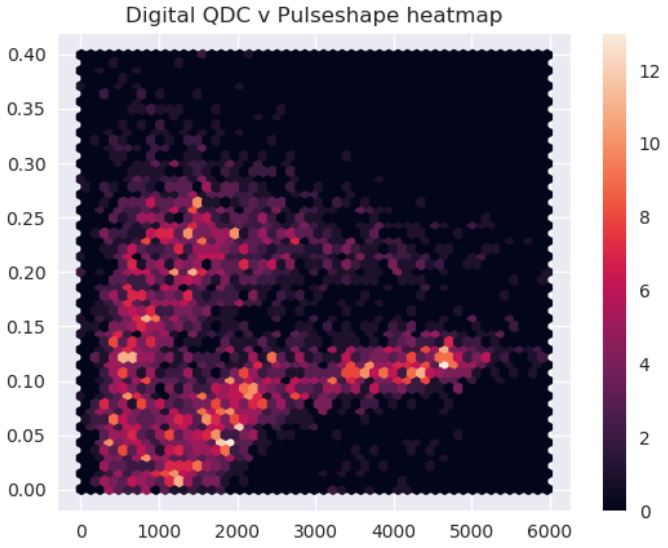

(a) Hexbin heatmap of Pulse shape distribution. The upper band is neutrons and the lower one is gammas.

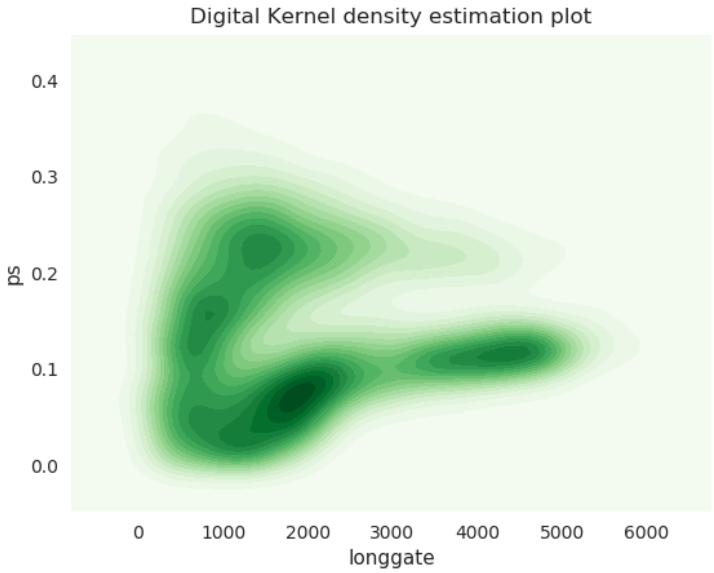

(b) Kernel density estimation plot of the pulse shape spectrum. The upper band is neutrons and the lower one is gammas.

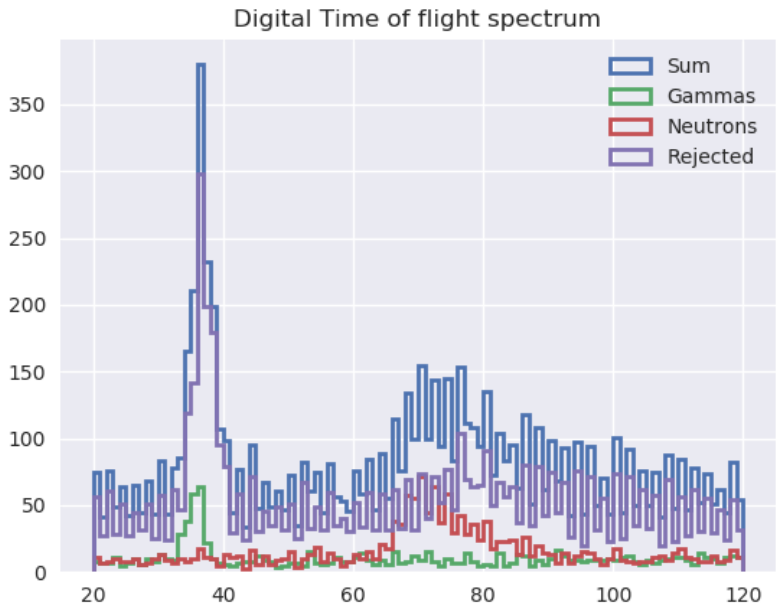

Figure 7: The digital time of flight spectrum, filtered using psd classification.

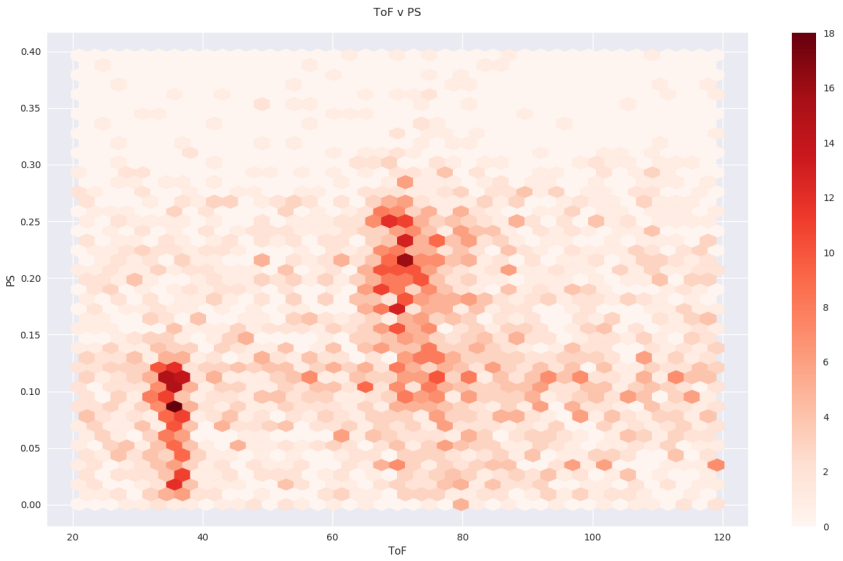

Figure 8: heatmap of ToF vs pulse shape.

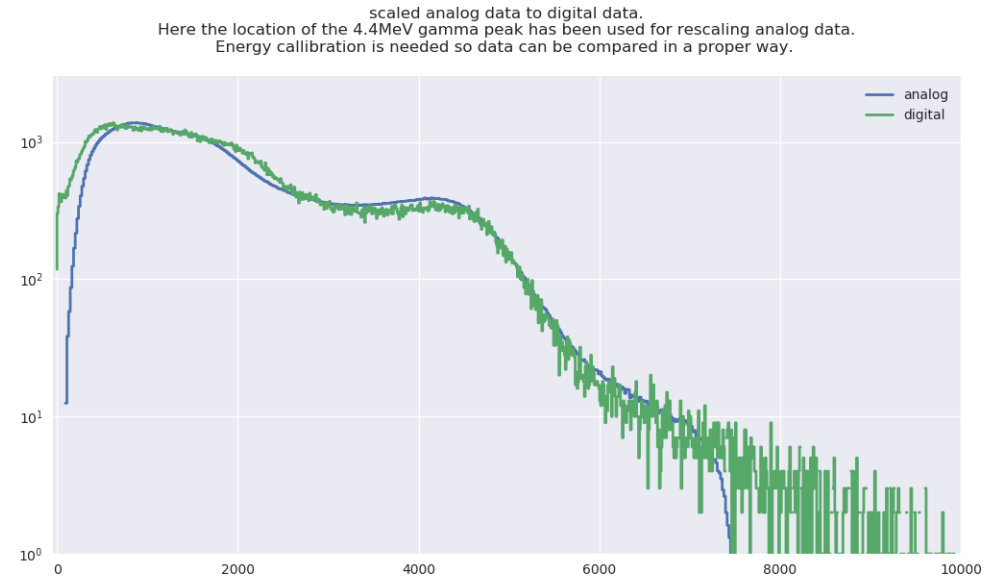

Figure 9: Analog and digital energy spectra